



Sizing and simultaneous quantification of nanoscale titanium dioxide and a dissolved titanium form by single particle inductively coupled plasma mass spectrometry



Janja Vidmar^{a,b}, Radmila Milačič^{a,b}, Janez Ščančar^{a,b,*}

^a Department of Environmental Sciences, Jožef Stefan Institute, Jamova 39, 1000 Ljubljana, Slovenia

^b Jožef Stefan International Postgraduate School, Jamova 39, 1000 Ljubljana, Slovenia

ARTICLE INFO

Article history:

Received 16 August 2016

Received in revised form 25 February 2017

Accepted 27 February 2017

Available online 2 March 2017

Keywords:

Nanoscale anatase

Nanoscale rutile

Single particle inductively coupled plasma mass spectrometry

Determination of size distribution

Simultaneous quantification of nanoscale and dissolved titanium forms

ABSTRACT

As a consequence of their widespread use, titanium dioxide nanoparticles (TiO₂NPs) have been released into the environment where they can act as stressors towards biota. For the assessment of the environmental impact of these NPs it is important to quantitatively determine their concentration, size distribution and the dissolved Ti fraction in different water samples. In the present work, a new analytical approach was applied for sizing and quantitative determination of TiO₂NPs (anatase and rutile) and dissolved Ti in aqueous samples by the use of single particle inductively coupled plasma mass spectrometry (SP-ICP-MS). The accuracy of the quantification of TiO₂NPs by SP-ICP-MS was verified by calculating the recoveries between the determined and expected Ti concentrations (90–100%). The size distributions of TiO₂NPs calculated by SP-ICP-MS (108 ± 10 nm for rutile, 29 ± 2 nm for anatase) were in a good agreement with data obtained by TEM (96–106 nm for rutile, 21–38 nm for anatase) and DLS (117 ± 22 nm for rutile, 42 ± 30 nm for anatase). The influence of different dwell times on the sizing and quantification of nanoscale titanium dioxide was also examined. Low limits of detection for NP diameter (37 nm) and NP concentration (3.69 × 10⁻³ ng Ti mL⁻¹ for rutile and 0.058 × 10⁻³ ng Ti mL⁻¹ for anatase) were obtained. In order to apply the procedure developed for the sizing and quantification of TiO₂NPs in environmental waters, the severe Ca isobaric interference at *m/z* 48 was overcome by measuring the Ti on *m/z* 47. It was demonstrated that the procedure optimized for the determination of Ti in environmental waters can be applied in the sizing and quantification of TiO₂NPs in river water samples spiked with nanoscale anatase and rutile.

© 2017 The Authors. Published by Elsevier B.V. This is an open access article under the CC BY-NC-ND license (<http://creativecommons.org/licenses/by-nc-nd/4.0/>).

1. Introduction

Titanium dioxide nanoparticles (TiO₂NPs) are the third most common nanomaterials and are used in a wide range of applications [1]. As a white pigment, they are added to foodstuffs, paints and coatings and are, due to their UV light resistant properties, used in photocatalytic sensors, pharmaceuticals and cosmetics, e.g., toothpaste and sunscreens [2]. Due to their increasing production and use, TiO₂NPs have been released into the environment, where their presence represents a potential health threat for living organisms. Many studies that have been performed *in vivo* and *in vitro* have shown several impacts of TiO₂NPs on algae, higher plants, aquatic and terrestrial invertebrates and freshwater fish. This is related to the formation of reactive oxygen species, causing oxidative stress in organisms and damaging lipids, carbohydrates, proteins and DNA [3–5]. Moreover, TiO₂NPs can enhance the uptake and toxicity of other pollutants (metal ions) [6]. Their toxic effects in biological systems largely depend on their concentration, surface

properties and size [7], as well as on the crystallinity of the TiO₂NPs. It has been demonstrated that only TiO₂NPs in the anatase crystalline phase induce the generation of reactive oxygen species [8], while the mixture of anatase and rutile causes mild DNA damage in human intestinal Caco-2 cells [9].

TiO₂NPs are likely to occur in the environment in the highest concentrations from among all engineered NPs. They can be found in treated wastewaters, sewage sludge, surface waters, sludge treated soils and sediments [10]. Detecting NPs in environmental samples is one of the greatest challenges due to their low concentrations in the environment (below ng L⁻¹) and complex matrices that can potentially change the NPs physico-chemical properties. Under different environmental conditions, such as pH, ionic strength and the presence of natural organic matter (NOM) or natural NPs, the aggregation, sedimentation and dissolution of NPs or their attachment to natural colloids can occur [11]. Multivalent cations, such as Ca²⁺, significantly reduce the NPs stability, while NOM, such as humic or fulvic substances, at low cation concentrations (low ionic strength) increases the stability of the NPs, preventing their aggregation [12]. Most TiO₂NPs have a point of zero charge (PZC) in the range of neutral pH values and thus aggregate rapidly in natural

* Corresponding author.

E-mail address: janez.scancar@ijs.si (J. Ščančar).

water samples [13]. Some NPs can also undergo dissolution reactions in the environment, which may cause a high local concentration of dissolved metal [5].

To follow the behaviour of NPs in the environment, a wide range of analytical procedures such as liquid chromatography (LC) and field flow fractionation (FFF) coupled to ICP-MS have been used for their sizing and quantification. As complementary techniques for determining the size distribution and the aggregation state of NPs, different microscopic techniques were applied [14–17]. These methods have some limitations in environmental applications, since the NPs concentrations in real samples are lower than their limits of detection and they require sample preparation and sample treatment during which the original NP properties can be altered. In order to separate the particulate and dissolved forms of the element, dialysis, filtration and ultracentrifugation can be used [18]. However, their limitation is the possible aggregation or adsorption of filtered NPs on the membrane surface [19].

As an alternative to separation procedures, a novel single particle SP-ICP-MS approach for the quantification and characterization of metal-containing NPs has been developed by Degueldre et al. [20–22]. The major advantages of SP-ICP-MS over other techniques for NP characterization and quantification are the minimal sample preparation, the superior sensitivity and the element specificity that may overcome complex matrices with background particles. SP-ICP-MS provides information about the NPs concentration and size distributions at mass concentration levels down to ng L^{-1} [23]. It also enables the simultaneous measurement of both the dissolved and particulate forms as well as a size distribution analysis for polydispersed NPs [24,25]. For SP-ICP-MS measurements, the suspensions of NPs need to be sufficiently diluted (ng L^{-1} level) and short integration times (10 ms or less) used in order to measure the intensity of a single particle as a single pulse. Under such conditions, the frequency of the pulses is proportional to the number concentration of NPs and the intensity of each pulse is related to the NP size. The SP-ICP-MS technique has so far been applied for the characterization of TiO_2 NPs [26] in wastewater effluent [27], surface water samples [28], drinking water [29] and in sunscreens [30].

To date, there are a lack of analytical procedures that would enable the characterization of TiO_2 NPs in environmental samples as well as the simultaneous quantification of nanoscale and dissolved Ti forms. Therefore, there is a need for reliable and sensitive analytical methods for the determination of TiO_2 NPs concentration and size distribution under environmental conditions. The aim of our work was to optimize the analytical procedure for sizing and the simultaneous quantification of TiO_2 NPs (anatase and rutile) and dissolved titanium by SP-ICP-MS and to apply the procedure to an analysis of environmental water samples.

2. Experimental

2.1. Instrumentation

SP-ICP-MS measurements were performed on a model 7900 ICP-MS instrument from Agilent Technologies (Tokyo, Japan) equipped with a quadrupole mass analyser. The operating parameters (summarized in Table 1) were optimized for plasma robustness and sufficient sensitivity.

For the stabilization of the TiO_2 NPs during the analytical procedure the samples were sonicated with an ultrasonic homogeniser, 4710 series, Cole-Parmer Instrument Co. (Chicago, IL, USA), equipped with a 6 mm diameter microprobe. It operated at a 10% power output and in the 50% pulsed operation mode for 3 min.

The morphology of the TiO_2 NPs powders was characterized using a transmission electron microscope (TEM) with an accelerating voltage of 200 kV (Jeol 2100, Tokyo, Japan). Prior to the TEM analysis, the investigated powders were dispersed in EtOH, deposited on a Cu TEM grid and dried in air.

Table 1
ICP-MS operating parameters for quantification and sizing of TiO_2 NPs by SP-ICP-MS.

Parameter	Type/value	Ti	Ag
Sample introduction			
Nebuliser	MicroMist		
Spray chamber	Scott		
Skimmer and sampler cone	Ni		
Sample depth	8 mm		
Nebulizer pump	0.3 rps		
Plasma conditions			
Forward power	1550 W		
Plasma gas flow		15.0 L min^{-1}	
Carrier gas flow (Ar)		0.98 L min^{-1}	
1.05 L min^{-1}			
Dilution gas flow (Ar)		0.3 L min^{-1}	
Makeup gas flow (Ar)			0.1 L min^{-1}
Collision gas flow (He)		4.3 mL min^{-1}	
Auxiliary gas flow	0.9 L min^{-1}		
Data acquisition parameters			
Data acquisition mode	TRA		
Integration time per isotope		3 ms, 5 ms, 10 ms	3 ms
Total acquisition time		30 s, 50 s, 100 s	30 s
Isotopes monitored		^{48}Ti , ^{47}Ti	^{107}Ag

The size distribution of the TiO_2 NPs was determined by dynamic light scattering (DLS) technique using Brookhaven NanoBrook OMNI Particle Size Analyser (Brookhaven Instrument Corporation, NY, USA). Prior to the DLS measurements, suspensions containing 0.2 mg/mL of rutile or 2 mg/mL of anatase were prepared in MilliQ water by the use of ultrasonication. The DLS characteristics of the measured samples were determined by averaging the results of three consecutive measurements (each in 10 runs) obtained for the one diluted working suspension.

A Mettler AE 163 (Zürich, Switzerland) analytical balance was used for all the weighings.

2.2. Materials and methods

Milli-Q water (18.2 $\text{M}\Omega\text{ cm}$) (Millipore, Bedford, MA, USA) was used for the sample preparations and sample dilutions. Standard TiO_2 NPs dispersions were prepared using anatase TiO_2 nanopowder (<25 nm particle size, spherical shape) (#637254) and rutile TiO_2 nanopowder (<100 nm particle size, rod shape with diameter of about 10 nm and length of 40 nm) (#637262) from Sigma-Aldrich (St. Louis, USA). The declared specific surface areas of the anatase and rutile were 45–55 $\text{m}^2\text{ g}^{-1}$ and 130–190 $\text{m}^2\text{ g}^{-1}$, respectively. The declared densities at 25 °C for the anatase and rutile were 3.9 g mL^{-1} and 4.17 g mL^{-1} , respectively. According to the manufacturer, the rutile nanopowder can contain up to 5 wt% silicon dioxide (SiO_2) as a surface coating.

Standard dispersions of silver NPs (AgNPs) with 20 and 40 nm diameters, purchased from Sigma-Aldrich (St. Louis, USA), and gold NPs (AuNPs) RM 8012 with 30 nm diameters, from NIST (Maryland, USA), were used for the determination of the transport efficiency. The AgNPs suspensions were supplied at a nominal concentration of $20 \pm 1\ \mu\text{g Ag L}^{-1}$ and were stabilized in an aqueous sodium citrate buffer, while the AuNP suspensions were supplied at a nominal concentration of $48.17 \pm 0.33\ \mu\text{g Au L}^{-1}$. The declared nominal sizes, determined by TEM, were $20 \pm 4\ \text{nm}$ and $40 \pm 4\ \text{nm}$ for the AgNPs and $27.6 \pm 2.1\ \text{nm}$ for the AuNPs. The AgNP and AuNP suspensions were made by diluting the stock solution with water to final concentrations ranging from 0.010 ng mL^{-1} to 2 ng mL^{-1} .

The dissolved Ti and Ag stock standard solutions (Merck) of $1000 \pm 4\ \text{mg L}^{-1}$ were used for the preparation of the calibration curves. They were prepared in 0.1% nitric acid in the concentration range from 0.010 ng mL^{-1} to 10 ng mL^{-1} .

2.3. Sample preparation

Approximately 10 mg of anatase or rutile were dispersed in 50 mL of water and sonicated for 3 min using an ultrasonic homogeniser with a probe. The suspensions were then immediately diluted in several subsequent dilution steps to obtain the final suspensions with a Ti concentration ranging from 0.001 to 1 ng mL⁻¹. All the experiments were performed in at least two replicates. The procedure for efficient dispersion of TiO₂NPs applied in the present study was previously optimized in our group [31]. Various procedures for stabilization of TiO₂NPs in solution (mechanical shaking, ultrasonication and the use of different dispersing agents e.g. PEI 600, Darvan C and Triton X-100) were examined. The results indicated that TiO₂NPs can be effectively dispersed in water by ultrasonic homogeniser with probe, or by combining ultrasonication and PEI 600 or Darvan C as dispersing agents. Nevertheless, for SP-ICP-MS measurements, dispersions of TiO₂NPs were prepared in water, since other dispersing agents have different transport efficiencies than aqueous NPs dispersions [32].

Since the microprobe's material of ultrasonic device is made from titanium, its potential contribution to the blank value was tested. Therefore, 50 mL of MilliQ water was ultrasonicated for 3 min, and TiO₂NPs and dissolved Ti were determined under the same conditions as the investigated samples (same dilution steps and instrumental parameters). The concentrations of the TiO₂NPs and the dissolved Ti determined in the blank were below the LODs, showing that microprobe does not contribute to the extraneous contamination.

To determine Ti mass concentration in river water spiked with anatase or rutile, previously developed microwave assisted digestion was applied [31]. Briefly, 10 mL of anatase or rutile suspension was transferred into 100 mL high-pressure Teflon vessel and 4 mL of HNO₃, 2 mL of HF and 1 mL of HCl were added. The sample was subjected to closed vessel microwave digestion (ramp to temperature 200 °C in 30 min, hold at 200 °C for 60 min). Then 6 mL of H₃BO₃ (4% aqueous solution) was added to dissolve fluorides and to complex the residual HF and contents again digested (ramp to temperature 200 °C in 15 min, hold at 200 °C for 30 min). Clear solution was quantitatively transferred to 50 mL graduated Teflon flask and appropriately diluted prior to the determination of Ti concentration by ICP-MS.

For sizing and quantification of the TiO₂NPs in environmental waters, a water sample, collected from the Sava River (Litija, Slovenia) during the first sampling campaign of the EU 7th FW funded GLOBAQUA project [33] in September 2014, was used. The samples were taken in 1 L polyethylene bottles and immediately transported to the laboratory. Since the river water contained a large amount of suspended particulate matter (62 mg L⁻¹), before the analysis both samples were filtered through 0.45 µm syringe CE filters (Minisart, Sartorius Stedim Biotech GmbH, Goettingen, Germany) in order to prevent the introduction of particulate matter into the ICP-MS system. Known amounts of anatase or rutile were then added to sample aliquots and the sample preparation for the SP-ICP-MS measurements was applied, as described above. In order to check whether TiO₂NPs are retained on the filters, filtration of nanoscale rutile and anatase suspensions was performed through 0.45 µm filters. It was found out that TiO₂NPs were not adsorbed on the filters.

2.4. SP-ICP-MS measurements

For the SP-ICP-MS measurements the data acquisition for the instrument was set to time-resolved-analysis (TRA) mode in order to collect the intensity for a single particle as it is vaporized and ionized in the plasma. The measurement duration for each run of TiO₂NPs and AgNPs was 100 s, 50 s or 30 s with a short integration dwell time of 10 ms, 5 ms or 3 ms per reading, respectively. The peristaltic pump was set to 0.3 rps for all the experiments, which corresponded to a sample flow rate of 0.996 ± 0.020 mL min⁻¹. The average flow rate was determined daily by weighing the amount of ultrapure water aspirated for

1 min. Ti and Ag in standard aqueous solutions were analysed at their most abundant isotopes ⁴⁸Ti (73.72%) and ¹⁰⁷Ag (51.84%), respectively. To overcome any possible polyatomic interferences from sulphur and nitrogen [34], the ⁴⁸Ti isotope was monitored in helium collision mode (4.3 mL min⁻¹ He gas flow). To demonstrate that the He mode contributes to a lower baseline, a comparison was made between the measurements of the ⁴⁸Ti isotope in the No gas mode and the He mode. As expected, a lower sensitivity of the measurement was obtained in the He mode (18.4 counts per µg Ti L⁻¹) than in the No gas mode (681 counts per µg Ti L⁻¹). However, due to the efficient removal of the polyatomic interferences, a lower baseline was obtained in the He mode, resulting in lower LODs for the dissolved and nanoscale Ti. Therefore, the He mode was chosen for all the experiments in the present study.

Since the ⁴⁸Ti isotope suffers from isobaric interferences of ⁴⁸Ca, an element commonly present in high concentrations in environmental waters, the less sensitive ⁴⁷Ti (7.3%) isotope was monitored in the river samples. The intensity data (counts per dwell-time interval as a function of time) were recorded using the ICP-MS Mass Hunter software, and exported to an Excel spreadsheet (Microsoft) for further data processing.

2.5. Determination of the transport efficiency of the NPs

Due to its low transport (nebulization) efficiency (η_{neb}), only a small fraction of the NP suspension reaches the ICP, where the particles are vaporized and ionized. When the NPs are sufficiently diluted, a single NP is detected by the ICP-MS as a single pulse or event. Establishing an accurate η_{neb} , defined as the ratio of the amount of analyte entering the plasma to the amount of analyte aspirated, is crucial for the quantification and sizing of NPs. In our study, the particle size method for the determination of η_{neb} described by Pace et al. was applied [35]. Intensity-mass calibration curves were established using Ag standards in dissolved form and reference monodispersed AgNPs with known particle sizes. The most common pulse intensities (i.e., the peak positions of the raw data histogram) were plotted against the total mass entering the sample introduction system. By assuming that nanoparticulate Ag behaves in the same way as dissolved Ag in the plasma, the ratio of the slope of the calibration curve of dissolved Ag (m_{diss}) over the slope of the calibration curve of particulate Ag (m_{NP}) will give the accurate η_{neb} . η_{neb} was measured daily and was found to be 4.7 ± 0.2%.

To check the accuracy of the transport efficiency determined by the AgNPs, the same experiments were also performed using AuNPs. Good agreement between the transport efficiencies determined by the AgNPs (5.3%) and the AuNPs (5.5%) was obtained.

3. Results and discussion

3.1. Size and size distribution of TiO₂NPs determined by TEM and DLS

In order to determine the size of two commercial TiO₂NPs powders, TEM images of nanoscale anatase and rutile were measured and are presented in Fig. S1 (Supplementary). The primary particles of rod shaped rutile observed in the TEM images have diameters between 24 and 30 nm and lengths between 96 and 106 nm (left-hand image). Observed is also the formation of aggregates larger than 160 nm (right-hand image). The primary particle size of spherical nanoscale anatase is between 21 and 38 nm (left-hand image) with aggregates larger than 100 nm (right image). The particle sizes of the rutile NPs determined by TEM are larger than those reported by the manufacturers (10 nm in diameter and 40 nm in length), which could be attributed to the NPs aggregation during storage.

The sizes and size distributions of the nanoscale rutile and anatase in aqueous solutions were further examined using the dynamic light scattering (DLS) method (Fig. S2) (Supplementary). The data from the DLS measurements were expressed as the average diameter for the size, and

the full-width-at-half maximum for the size distribution. The DLS measurements indicate that nanoscale rutile dispersed in water using ultrasonication has average diameters of 33 ± 6 nm and 117 ± 22 nm, and aggregates with diameters larger than 170 nm. For nanoscale anatase the size distribution with an average diameter of 42 ± 30 nm was determined. Considerable aggregation also occurred, which was evident from two larger peaks (100 to 300 nm and 1000 to 3000 nm). The data on the size and the size distributions of the

nanoscale rutile and anatase obtained by DLS are in good agreement with the sizes determined by TEM.

3.2. Determination of TiO_2 NPs size and size distribution by SP-ICP-MS

The intensity of the pulse generated by a single NP and detected by ICP-MS can be related to the NP size only if the composition, shape and density of the NP are known. Ideally, for the most accurate

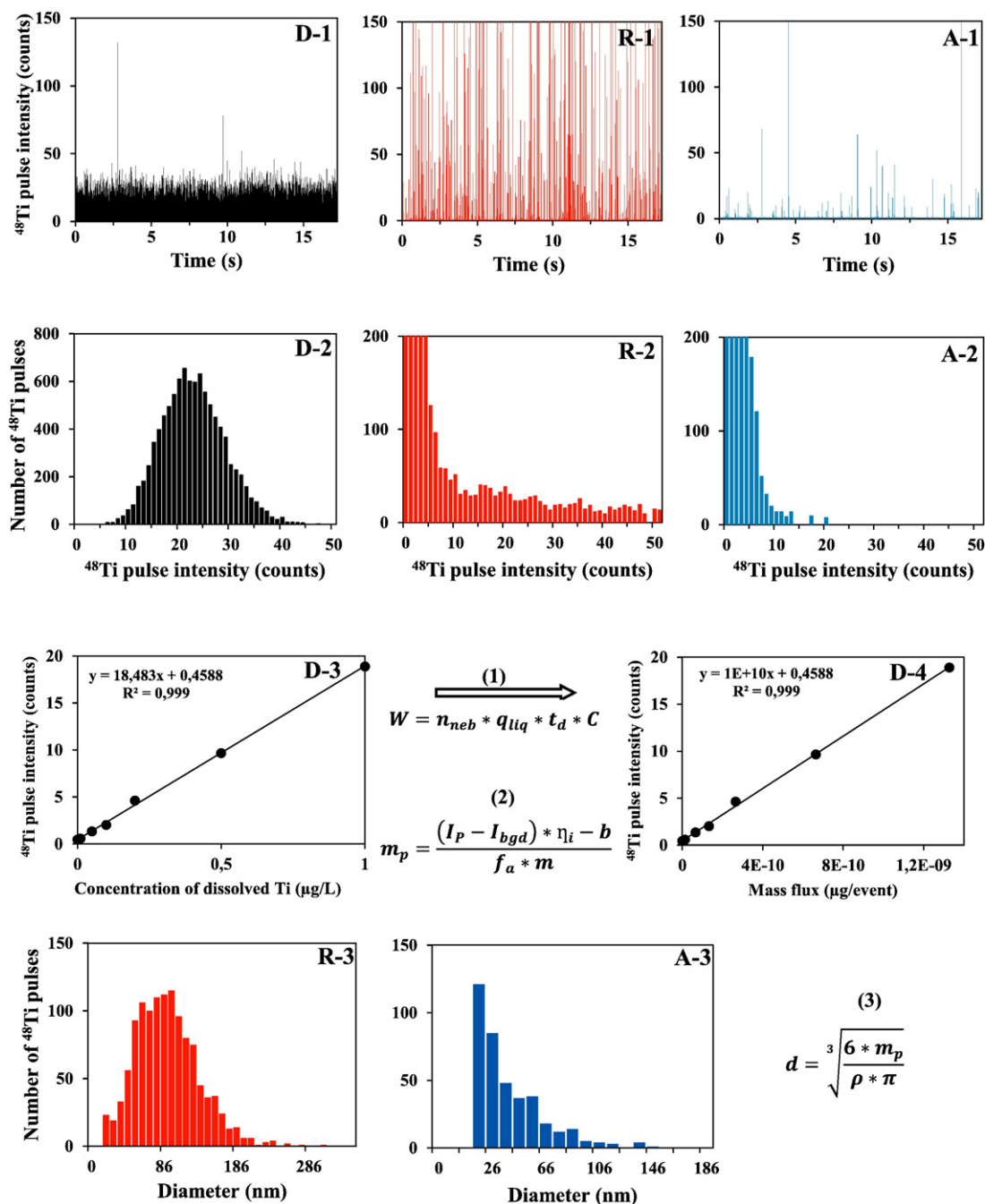


Fig. 1. Data processing for the determination of the size distribution of TiO_2 NPs using SP-ICP-MS. Time scans for dissolved Ti ($0.5 \text{ ng Ti mL}^{-1}$) (D-1), TiO_2 NPs in rutile ($0.2 \text{ ng Ti mL}^{-1}$) (R-1) and anatase ($0.6 \text{ ng Ti mL}^{-1}$) (A-1); corresponding signal distribution histograms for dissolved Ti (D-2), TiO_2 NPs in rutile (R-2) and anatase (A-2); calibration curve (dissolved Ti standards) created for particle size calculation (D-3); calibration curve created for the calculation of the mass of an individual particle (D-4); size distribution histograms for TiO_2 NPs in rutile (R-3) and anatase (A-3). SP-ICP-MS measurements were performed at 10 ms dwell time (the schematic presentation is adapted from ref. [34], while the data are from the present work). Symbols b – interception of the mass flux calibration curve with ordinate (count) C – dissolved Ti mass concentration ($\mu\text{g L}^{-1}$) d – particle diameter (nm) f_a – molar fraction of metal in the nanoparticle I_{bgd} – signal intensity of the background (count) I_p – signal intensity of a particle (count) m – slope of the mass flux calibration curve (count event μg^{-1}) m_p – mass of a particle ($\mu\text{g event}^{-1}$) q_{liq} – sample flow rate (mL min^{-1}) t_d – dwell time (ms) t_i – acquisition time (s) W – mass flux ($\mu\text{g s}^{-1}$) η_i – ionization efficiency η_{neb} – transport efficiency ρ – particle density (g mL^{-1}).

determination of NPs size by SP-ICP-MS, reference nanoparticles with well-characterized properties of the same elemental composition as sample analysed should be used. However, for TiO₂NPs no suitable reference materials in monodispersed form with well-characterized size exist. Therefore, for sizing, dissolved Ti standards were used to prepare a calibration curve by plotting the mass concentration versus the signal intensity of the dissolved Ti solutions. The procedure applied in our study is a well-known and widely used by numerous researchers for different NPs types [26–30,35–37]. To obtain a time scan, a solution of dissolved ⁴⁸Ti was measured by SP-ICP-MS (Fig. 1).

The time scan (Fig. 1, D-1) was converted into a signal distribution histogram (Fig. 1, D-2) and the most common Ti pulse intensity was plotted versus the concentration of dissolved Ti (Fig. 1, D-3) in order to create the calibration curve. The Ti mass concentration was then converted into the total mass transported into the plasma, the mass flux (W), through the transport efficiency (η_{neb}), the sample flow rate (q_{liq}), the dwell time (t_d) and the Ti mass concentration (C) using Eq. (1) (Fig. 1, D-4). η_{neb} was determined using standard AgNPs, as described in the Section 2.5. Determination of transport efficiency of NPs. The slope of the calibration curve in Fig. 1 D-4 and its interception with the ordinate were inserted into Eq. (2) for the calculation of the mass of an individual particle.

Time scans of the TiO₂NPs in rutile (Fig. 1, R-1) and anatase (Fig. 1, A-1) were measured and converted into signal distribution histograms (Fig. 1, R-2, A-2). Before sizing, the background intensity was subtracted from the TiO₂NPs pulse intensity. The most important contribution to the background intensity arises from the dissolved component of the element in the solution, isobaric and/or polyatomic interferences (if these are not adequately eliminated) and the instrument background. A criterion based on three times the standard deviation of the continuous background was selected for the discrimination of the NPs pulses from the background [23]. First, the full data set was averaged, and pulses above 3σ (standard deviation) were separated. This process was subsequently repeated, until the baseline concentration remained at a constant value. Then, once the baseline was established, pulses above 3σ were gathered and defined as NPs. Finally, in order to calculate the particle mass (m_p), the average background intensity (I_{bgd}) was subtracted from the individual pulse intensities (I_p) of the TiO₂NPs dataset (Fig. 1, A-2, R-2) and inserted into Eq. (2) along with the ionization efficiency (η_i) and the molar fraction of the metal in the nanoparticle (f_d). Each particle mass was then converted into a particle diameter (d) with the use of the particle density (ρ) in Eq. (3), which enabled to create a size distribution histogram (Fig. 1, R-3, A-3) [35].

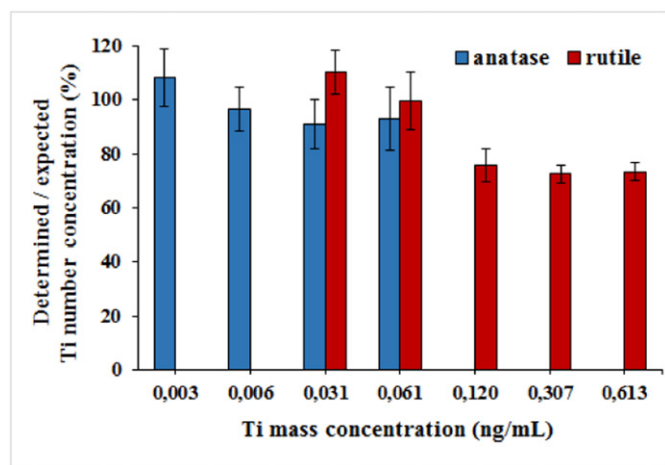


Fig. 2. Ratio between the determined and expected Ti mass concentrations as a function of Ti mass concentration for anatase and rutile TiO₂NPs, measured by SP-ICP-MS at 10 ms dwell time. Results represent the mean value of three replicates with the standard deviation of the measurements.

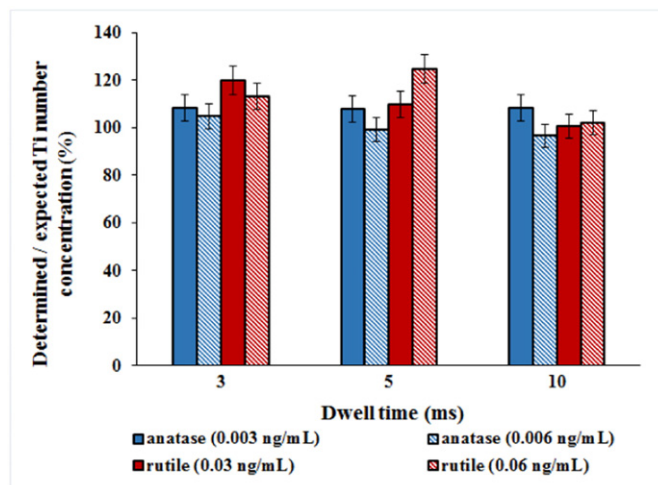


Fig. 3. Ratio between the determined and expected Ti mass concentrations as a function of dwell time for two Ti mass concentrations (0.003 and 0.006 ng Ti mL⁻¹ for anatase and 0.03 and 0.06 ng Ti mL⁻¹ for rutile) of TiO₂NPs measured by SP-ICP-MS. Results represent the mean value of three replicates with the standard deviation of the measurements.

It is clear that a large number of pulses above the background are obtained for anatase (Fig. 1, A-1) and rutile (Fig. 1, R-1) NPs, whereas a continuous background signal with only a few single pulses can be seen for the dissolved Ti (Fig. 1, D-1). Namely, dissolved Ti is continuously introduced into the plasma, where a constant number of atoms are ionized and detected, while the TiO₂NPs in a sufficiently diluted suspension are not homogeneously distributed. Therefore, only a small fraction of aerosol droplets containing one NP are aspirated into the plasma, ionized into the packet of ions and detected as a single pulse. The lower intensity of pulses for the TiO₂NPs in anatase (Fig. 1, A-1) in comparison to rutile (Fig. 1, R-1) is related to the smaller NPs in the anatase. From the data in Fig. 1 (R-3 and A-3), where the SP-ICP-MS measurements were performed at 10 ms dwell time, the mean diameters for the TiO₂NPs in the rutile and anatase were calculated to be 108 ± 10 nm and 29 ± 2 nm, respectively (expressed as an average of three replicates with the standard deviation of the measurements). The corresponding full-width-at-half-maximum for the size distribution of the nanoscale rutile was 90 nm. Since the size distribution of the nanoscale anatase towards smaller particle sizes is below the size LOD, the half-width instead of the full-width-at-half-maximum was determined and calculated to be 15 nm.

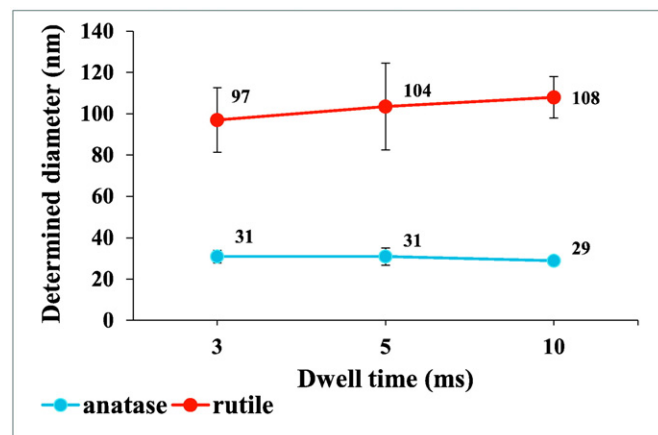


Fig. 4. Influence of dwell time on the determination of the mean diameter of TiO₂NPs in anatase (declared size 25 nm) and rutile (declared size 100 nm) by SP-ICP-MS. Results represent the mean value of three replicates with the standard deviation of the measurements.

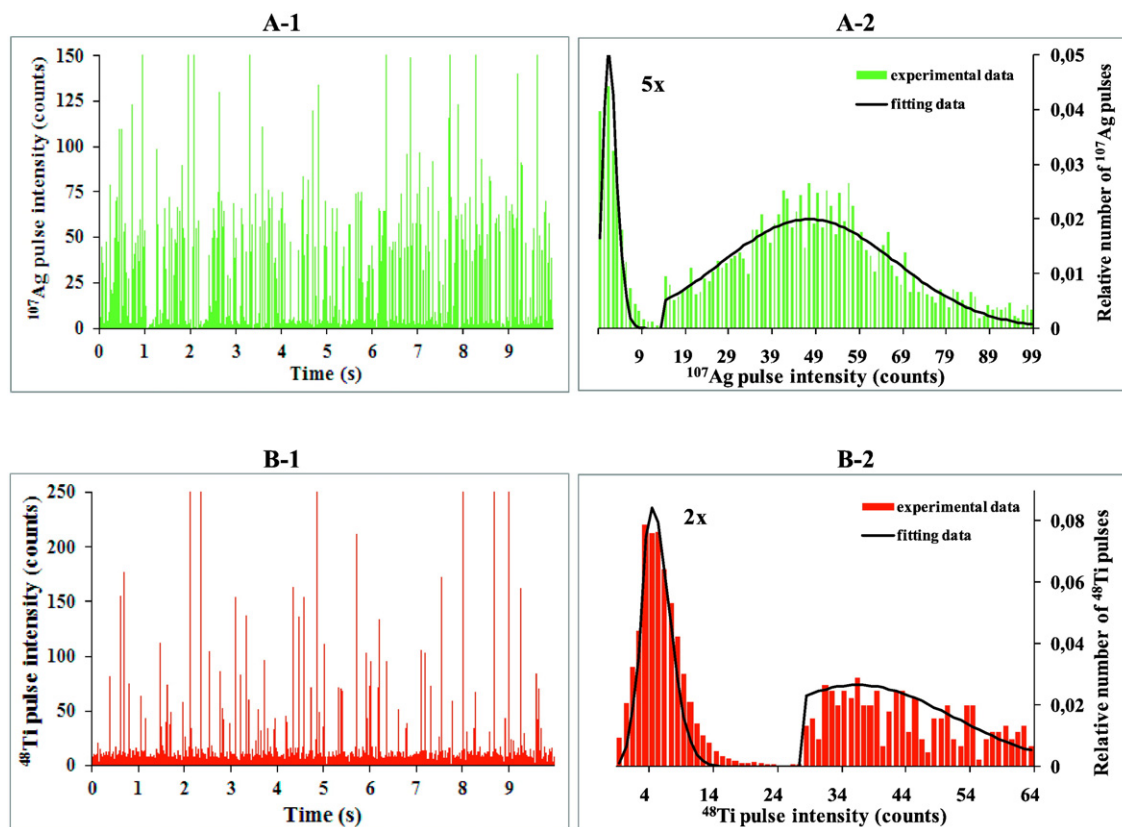


Fig. 5. Time scans (A-1, B-1) and signal distribution histogram (A-2, B-2) for the mixture of 40 nm AgNPs ($0.5 \text{ ng Ag mL}^{-1}$) and dissolved Ag ($0.5 \text{ ng Ag mL}^{-1}$) and the mixture of TiO_2 NPs ($0.3 \text{ ng Ti mL}^{-1}$, rutile) and dissolved Ti ($0.5 \text{ ng Ti mL}^{-1}$), respectively. Measurements were performed by SP-ICP-MS at 3 ms dwell time for the AgNPs and 10 ms for the TiO_2 NPs. Signals from the dissolved form of the element are fitted to a Poisson distribution, while signals from the particulate form of the element are fitted to a Gaussian distribution.

The diameters and the full-width-at-half maximum for the rutile and anatase determined with the SP-ICP-MS analysis are in a good agreement with the sizes and size distributions obtained from the TEM and DLS measurements. The peak tailing towards larger particle sizes is associated with the formation of larger particles due to the NPs aggregation. This observation is in accordance with the aggregates observed in the TEM and DLS measurements. However, aggregates with sizes larger than 100 nm for anatase and larger than 160 nm for rutile, determined with the TEM and DLS analysis, were not observed using SP-ICP-MS. Namely, the upper size limit for the particle diameter in the SP-ICP-MS is limited by the selective removal of large particles in the spray chamber or their incomplete vaporization in the plasma [36]. On the other hand, the wide size distribution in the histogram of rutile towards the smaller particle sizes indicates the polydispersed nature of the TiO_2 NPs in rutile. While TEM and DLS analysis can distinguish between the diameter and length of the rod-shaped rutile NPs, signal in SP-ICP-MS analysis carries no information about two dimensions of non-spherical NPs. Therefore, the mean diameter of rod-shaped

nanoscale rutile determined by SP-ICP-MS was calculated assuming a spherical particle shape.

3.2.1. Nanoparticle diameter limit of detection

The NP diameter limit of detection (LOD_d) is related to the capability of a NP to produce a pulse with a number of counts equal to three times the standard deviation (σ) of the background (Milli-Q water) [24]. From the background signals (2 counts per 10 ms dwell time) with standard deviations of 1 count, the theoretical LOD_d was calculated and found to be 37 nm. Nevertheless, from the size distribution histograms for the TiO_2 NPs in the anatase and rutile crystalline phases (Fig. 1, A-3 and R-3) it is evident that sizing of the TiO_2 NPs is possible, even for particles smaller than 37 nm. Alternatively, for calculating the LOD_d the smallest pulse height that can be distinguished from the background was considered [36], and a similar LOD_d (34 nm for TiO_2 NPs) was obtained. Similar LOD_d for TiO_2 NPs determined at ^{48}Ti isotope was reported by Dan et al. [30].

Table 2
Recoveries between determined and expected mass concentrations for the simultaneous determination of the Ti mass concentration in TiO_2 NPs and dissolved Ti by SP-ICP-MS. Results represent the mean value of three replicates with the standard deviation of the measurements.

	TiNP added (ng mL^{-1})	Ti(IV) added (ng mL^{-1})	TiNP measured (ng mL^{-1})	Ti(IV) measured (ng mL^{-1})	Recovery TiNP (%)	Recovery Ti(IV) (%)
Rutile	0.298 ± 0.006	0.500 ± 0.005	0.298 ± 0.034	0.456 ± 0.031	100	91
	0.0323 ± 0.0006	0.050 ± 0.001	0.0312 ± 0.0024	0.047 ± 0.003	97	94
Anatase	0.580 ± 0.012	0.500 ± 0.005	0.480 ± 0.020	0.525 ± 0.024	83	105
	0.348 ± 0.007	0.500 ± 0.005	0.320 ± 0.064	0.470 ± 0.038	92	94
	0.0580 ± 0.0012	0.050 ± 0.001	0.0562 ± 0.0010	0.0558 ± 0.0007	97	112
	0.0348 ± 0.0007	0.050 ± 0.001	0.0301 ± 0.0033	0.0628 ± 0.001	87	126

3.3. Quantitative determination of Ti number concentration in anatase and rutile

In order to evaluate the capability of the SP-ICP-MS method to quantitatively determine the Ti number concentration in TiO₂NPs, dispersions of anatase and rutile with different Ti mass concentrations (0.003–0.6 ng mL⁻¹) were prepared. First, the mean dissolved background intensity was subtracted from the pulse intensity using the 3 σ criterion. The particle number concentration was determined by dividing the frequency of the pulse events by the sample flow rate and the transport efficiency. The recoveries, defined as the ratio between the determined and expected Ti number concentrations in the TiO₂NPs, were calculated and are presented in Fig. 2.

As evident, with increasing Ti concentrations, the recoveries are decreasing, and for the anatase they lie between 108 and 91%, while for the rutile they are between 110 and 73%. Namely, at higher NP concentrations the occurrence of multiple particle events, which are each counted as a single particle event, is increasing. With an increasing Ti concentration, the background signal is also increased, which makes it difficult to detect TiO₂NPs that produce signals near the background [18]. These phenomena led to an underestimation of the particle concentrations, regardless of their size (anatase or rutile). For this reason, it is important that the number of particles entering the plasma in one dwell time is controlled by the appropriate sample flow rate and/or dilution.

3.3.1. Nanoparticle concentration limit of detection

The number concentration limit of detection (LOD_{NP}) is related to the capability of counting three NP events using Eq. (1) [36]:

$$\text{LOD}_{\text{NP}} = 3 \times \frac{1}{\eta_{\text{neb}} q_{\text{liq}} t_i} \quad (1)$$

From Eq. (1) it is evident that a lower LOD_{NP} can be achieved by improving the transport efficiency, increasing the sample flow rate, and/or using longer acquisition times. However, the flow rates should be carefully adjusted to prevent multiple particle events and reasonable acquisition times should be chosen. The LOD_{NP} for TiO₂NPs calculated using Eq. (1) was found to be 2.3×10^5 NPs L⁻¹. To convert the LOD_{NP} to the mass concentration limits of detection, the size as well as the composition and density of each type of TiO₂NPs were considered and the calculated LOD_{NP} corresponded to 3.69×10^{-3} ng Ti mL⁻¹ for rutile and 0.058×10^{-3} ng Ti mL⁻¹ for anatase.

3.4. Influence of dwell time on the determination of the number concentration and size distribution of TiO₂NPs

For the accurate detection of NPs by SP-ICP-MS, the dwell time should be carefully selected. It should be long enough to collect the entire signal from one NP and to ensure that the measurement of one NP is not divided between two consecutive dwell times. The partial measurement of a NP would lead to an underestimate of the particle size and an overestimate of the particle number concentration. A sufficiently long dwell time is also important for ensuring an accurate discrimination of the NP signal from the background signal [27]. On the other hand, the dwell time should be short enough to avoid the measurement of two NPs in a single integration period, which would lead to an overestimation of the size of the NPs, and an underestimation of the particle number concentration [18,23].

In order to evaluate the influence of different dwell times on the quantification of TiO₂NPs by SP-ICP-MS, dwell times of 3, 5 and 10 ms were applied in measurements of the number concentrations and size distributions of the anatase and rutile. Aqueous suspensions of anatase and rutile at different Ti mass concentrations (0.003 and 0.006 ng mL⁻¹ for anatase and 0.03 and 0.06 ng mL⁻¹ for rutile) were prepared and measured at different dwell times (Fig. 3). The Ti number concentrations were determined and the recoveries between the

determined and expected Ti in the TiO₂NPs were calculated as described in the Section 3.3. Quantitative determination of Ti number concentration in anatase and rutile.

From Fig. 3 it is evident that with shorter dwell times the estimated Ti number concentration and consequently the measured recoveries are increasing for the anatase and rutile. As expected, 3 and 5 ms dwell times are too short for measuring the anatase and rutile for the investigated TiO₂NPs concentrations, since particle events within a single dwell period are only partially measured. The dwell time also affects the analytical performance of the dissolved Ti fraction. The LODs for

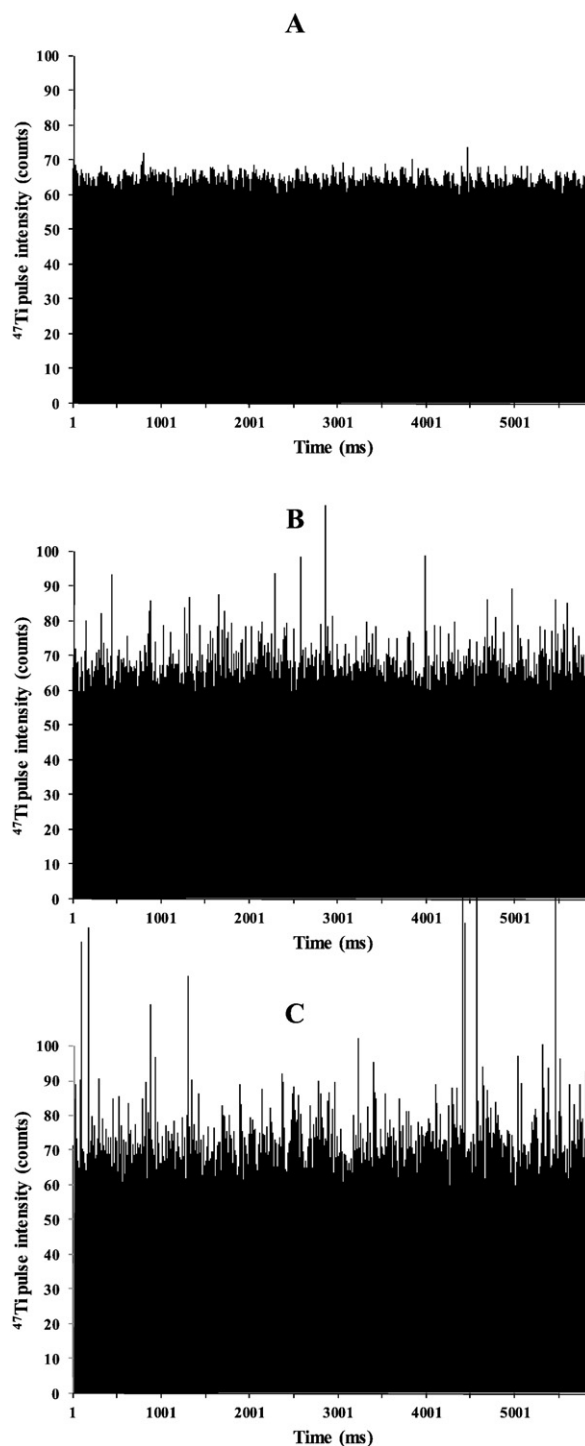


Fig. 6. Time scans of river water sample (A), sample spiked with rutile (0.0256 ng Ti mL⁻¹) (B) and sample spiked with anatase (0.00113 ng Ti mL⁻¹) (C). SP-ICP-MS measurements were performed at 10 ms dwell time.

Table 3
Simultaneous determination of the mass concentration of dissolved Ti and TiNPs in a river water sample by SP-ICP-MS and recoveries between the determined and expected mass concentrations in a sample spiked with TiO₂NPs (anatase and rutile). Results represent the mean value of three replicates with the standard deviation of the measurements.

Sample/spiked sample	TiNP added (ng mL ⁻¹)	Ti(IV) measured (ng mL ⁻¹)	TiNP measured (ng mL ⁻¹)	Recovery TiNP (%)
River water	/	0.588 ± 0.022	<0.0001	/
Rutile	0.0256 ± 0.0005	0.581 ± 0.030	0.0267 ± 0.0013	104
Anatase	0.00113 ± 0.00002	0.585 ± 0.037	0.00156 ± 0.00008	138

the dissolved Ti fraction, which were determined at 3, 5 and 10 ms dwell times, were calculated to be 0.101, 0.071 and 0.045 ng Ti mL⁻¹, while the slopes of the calibration plots for the dissolved Ti were 28.4, 26.2 and 18.4 counts per µg Ti L⁻¹, respectively. Therefore, a 10 ms dwell time was selected due to the lowest LOD, despite the reduced sensitivity for the determination of the Ti at this dwell time.

The influence of different dwell times on the particle size of TiO₂NPs in anatase and rutile determined by SP-ICP-MS was also evaluated. Dispersions of anatase and rutile were prepared at different Ti concentrations and measured at 3, 5 and 10 ms dwell times. The mean diameters were calculated from the size distribution histograms, following the procedure described in the Section 3.2. Determination of TiO₂NPs size and size distribution by SP-ICP-MS. The results are presented in Fig. 4.

As is evident from Fig. 4, the mean diameters, which represent the average value of five replicates with the standard deviation of the measurements, are close to those observed in the TEM images. The dwell times do not have a significant influence on the determined mean diameters for the anatase and rutile NPs, despite the expected particle splitting between subsequent measurements, which may lead to an underestimation of the mean diameters if the dwell times are too short. However, a 10 ms dwell time was selected for the quantification and sizing of the TiO₂NPs and the dissolved Ti by SP-ICP-MS due to the better recoveries for the NPs mass concentration and the lower LOD for the dissolved Ti fraction at longer dwell times.

3.5. Simultaneous quantification of TiO₂NPs and dissolved Ti

In an evaluation of the biological effects of TiO₂NPs it is necessary to distinguish between the dissolved Ti ions and the nanoscale TiO₂. In environmental water samples, considerable concentrations of dissolved Ti, which originate from the soluble Ti compounds, can be present as a natural background. Although Ti is the ninth-most abundant element in the Earth's crust, it is present in natural water in very low concentrations due to its very low mobility under almost all environmental conditions. However, some dissolved Ti may be released into stream water through the weathering of ferromagnesian minerals, anatase, etc. The Ti concentrations in natural water can range from <0.01 to 16.8 µg L⁻¹, with a median value of 0.9 µg L⁻¹ [37].

Since there are no adequate monodispersed TiO₂NP standards available, the capability of SP-ICP-MS for simultaneous quantification of nanoscale and dissolved metal forms was first verified by an analysis of the monodispersed AgNPs with a 40 nm size in the presence of dissolved Ag. In Fig. 5 an example of a time scan (A-1) and a signal distribution histogram (A-2) for 0.5 ng mL⁻¹ of AgNPs in the presence of 0.5 ng mL⁻¹ of dissolved Ag are presented. The SP-ICP-MS measurements were performed at 3 ms dwell time.

In the signal distribution histogram (Fig. 5, A-2), first, the distribution for low-intensity signals, which represents the dissolved Ag and background, was fitted to the Poisson distribution, assuming that the ions randomly reach the detector. The second distribution, which was fitted to the Gaussian distribution, represents the AgNPs [39]. Once the dissolved and NP fractions had been resolved, each fraction was quantified by summing the number of counts for each distribution obtained in the histograms. Before the integration of the NP fraction, the mean dissolved background intensity was subtracted from the pulse intensity. The integration data was then compared with the calibration curve obtained with the use of dissolved Ag standards and the mass concentrations for Ag in the particulate and dissolved form were calculated [24]. The ratio between the determined and expected Ag mass concentrations was found to be 95% for AgNPs and 98% for dissolved Ag.

The same approach was then applied for the simultaneous quantification of TiO₂NPs and dissolved Ti. For this purpose, dispersions of nanoscale anatase and rutile in different concentrations, to which dissolved Ti was added, were prepared. In Fig. 5, B-1 the time scan for the mixture of rutile (0.3 ng Ti mL⁻¹) and dissolved Ti (0.5 ng Ti mL⁻¹) is presented, indicating the presence of TiO₂NP pulses and a continuous background of dissolved Ti. The relative numbers of pulses (numbers of pulses divided by the total number of NP events) were plotted against pulse intensity, creating a signal distribution histogram (Fig. 5, B-2). The well-resolved distributions for the dissolved and particulate forms were fitted to Poisson and Gaussian functions, respectively, and the mass concentrations of the dissolved Ti and TiO₂NPs were calculated.

The results of the recovery tests for the simultaneous determination of the Ti mass concentrations in anatase and rutile TiO₂NPs and the dissolved Ti are presented in Table 2.

The data from Table 2 demonstrate that the recoveries for nanoscale rutile range from 97 and 100%, and for dissolved Ti from 91 to 94%. It can

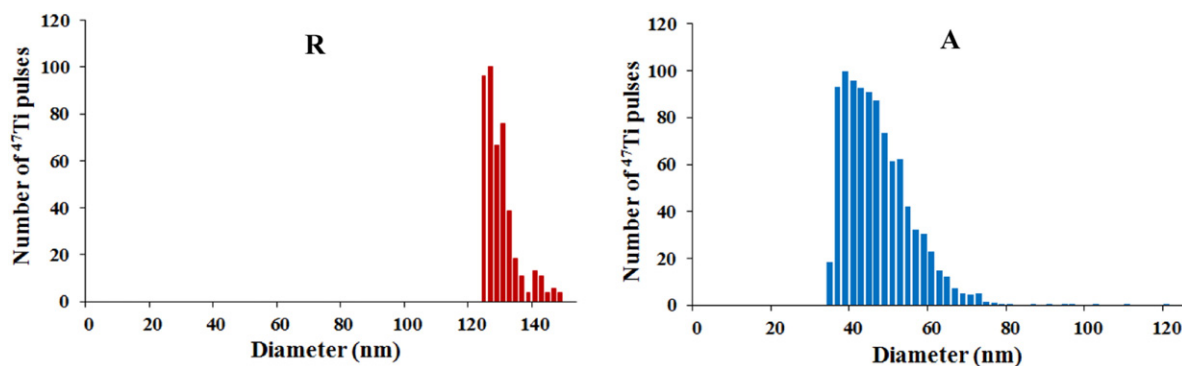


Fig. 7. Size distribution histograms for rutile TiO₂NPs (0.103 ng Ti mL⁻¹) (R) and for anatase TiO₂NPs (0.00113 ng Ti mL⁻¹) (A) dispersed in river water. SP-ICP-MS measurements were performed at 10 ms dwell time.

be further seen that for anatase these recoveries are between 83 and 97% for the nanoscale Ti form and between 94 and 126% for the dissolved Ti form. In general, the lower recoveries for TiO₂NPs in anatase in comparison to rutile may be attributed to the smaller size of the NPs that can be partially overlapped with the dissolved Ti background, which makes the discrimination of the dissolved and nanoparticulate forms more difficult. For the same reason, recoveries higher than 100% were observed for the dissolved Ti.

3.6. Quantification and sizing of TiO₂NPs in river water samples

In order to assess the applicability of the procedure developed for the sizing and quantification of TiO₂NPs in environmental waters, a river water sample was collected and prepared as described in the Section 2.3. Sample preparation. It contained 38 mg Ca L⁻¹, which causes severe isobaric interferences in the determination of Ti at *m/z* 48. To avoid this type of interferences, the Ti concentrations in the river water measured by ICP-MS and SP-ICP-MS were performed at *m/z* 47, while the He mode was applied to compensate for possible polyatomic interferences [33]. The theoretical LOD_d determined for TiO₂NPs at ⁴⁷Ti isotope (7.3% abundance) was found to be 55 nm and is higher than LOD_d determined at the most abundant ⁴⁸Ti isotope (73.72% abundance) (37 nm) (see data in Section 3.2.1). Namely, the use of more abundant isotope contributes to the higher sensitivity and consequently to the lower LOD_d. In the literature, LOD_d determined at ⁴⁷Ti or ⁴⁹Ti isotopes ranged from 65 to 100 nm [26,29,36,37]. Lower LOD_d determined at ⁴⁷Ti in the present study is related to the low baseline due to the use of He gas that effectively removes polyatomic interferences in ICP-MS determination.

The total Ti concentration in the river water determined by ICP-MS was found to be 0.602 ± 0.012 ng Ti mL⁻¹, which is within the range reported for other natural waters [38]. In order to determine the dissolved and nanoparticulate fractions of Ti in the river water SP-ICP-MS analysis was carried out. The time scan of the river water sample is presented in Fig. 6, A.

Due to the increased signal intensity of the dissolved Ti in the river water, which can be seen in the elevated background (enlarged time scans in Fig. 6), the overlap of the signals for the NPs and the dissolved fraction is more pronounced. Therefore, to distinguish between the dissolved and nanoscale Ti, the 5 σ criterion was chosen [27] and the mass concentrations were determined as described in the Section 3.5. Simultaneous quantification of TiO₂NPs and dissolved Ti. The concentration of dissolved Ti was 0.588 ± 0.022 ng Ti mL⁻¹, while nanoscale Ti was found to be below the LOD_{NP} (<0.0001 ng mL⁻¹), since no sources of titania, e.g. industrial activities or release of nano titania from sunscreens (swimming in the river), were present in the vicinity. To evaluate the influence of the sample matrix on the determination of the TiO₂NPs mass concentration and their size, the river water was spiked with different concentrations of rutile (0.0256 ng Ti mL⁻¹) and anatase (0.00113 ng Ti mL⁻¹). Corresponding time scans, which clearly indicate the appearance of TiO₂NP pulses and the continuous background of dissolved Ti present in the river water, are presented in Fig. 6, B and C, while the recoveries calculated as the ratio between the determined and expected TiNPs concentrations are presented in Table 3.

The expected Ti mass concentrations were determined after the microwave assisted digestion of the TiO₂NP suspensions [31]. It is evident that the addition of TiO₂NPs to the river water has no influence on the quantification of the dissolved Ti originally present in the sample. Good recoveries were obtained for the nanoscale rutile (104%), while for anatase, with the smaller NPs, the higher recoveries (138%) are most likely related to the contribution of the dissolved Ti background to the NPs signal.

For the sizing of the TiO₂NPs added to the river water, it was necessary to accurately determine the transport efficiency. For this purpose, monodispersed AgNPs (40 nm) and dissolved Ag standard solutions were prepared in the river water and the transport efficiency calculated

as described in the paragraph 2.5. Determination of transport efficiency of NPs. η_{neb} for the river water was found to be 3.9 ± 0.2%. Following the procedure described in the Section 3.2. Determination of TiO₂NPs size and size distribution by SP-ICP-MS, size distribution histograms for the rutile and anatase in river water were created (see Fig. 7) and the mean diameters were calculated.

For the rutile added to the river water the mean diameter was found to be 128 nm, while for anatase it was 44 nm. Although the theoretical LOD_d (55 nm) is higher than the mean diameter of anatase determined in the river water, it is evident that sizing of the TiO₂NPs is possible even for smaller particles. Slightly larger diameters than those determined for the rutile and anatase dispersed in Milli-Q water (108 and 29 nm, respectively) can be attributed to the NPs aggregation due to the ionic strength of the river water.

4. Conclusions

Instrumental parameters were optimized for an accurate sizing and simultaneous quantification of TiO₂NPs (anatase and rutile) and dissolved Ti by SP-ICP-MS. Since there is no standard for monodispersed TiNPs with a reference value for the NPs size, η_{neb} was determined using a reference monodispersed AgNP standard. The influence of dwell time on the sizing and quantification of the TiO₂NPs and the dissolved Ti fraction was critically evaluated. The optimal dwell time was found to be 10 ms. Good recoveries between the determined and expected TiNPs mass concentrations and the calculated size distributions of the TiO₂NPs in anatase and rutile, which agreed well with the sizes determined from TEM and DLS measurements, confirmed the accuracy of the developed SP-ICP-MS procedure. The method also enables simultaneous quantification of the nanoscale and dissolved Ti forms. To overcome severe Ca isobaric interference with Ti at *m/z* 48, the ⁴⁷Ti isotope was used in the analysis of the river water samples. It was demonstrated that the procedure optimized for the determination of Ti in environmental waters can be applied in the sizing and quantification of TiNPs in river water samples spiked with nanosize TiO₂. The concentration of dissolved Ti in the Sava River (Litija) was 0.588 ± 0.022 ng Ti mL⁻¹, whereas nanoscale Ti was below 0.0001 ng mL⁻¹, indicating that there were no sources of titania at this sampling point. At industrially exposed sites or bathing resorts, the nanoscale Ti can be present in measurable concentrations and determined by SP-ICP-MS.

Supplementary data to this article can be found online at <http://dx.doi.org/10.1016/j.microc.2017.02.030>.

Acknowledgments

This work has been supported by the European Communities 7th Framework Programme Funding under Grant agreement no. 603629-ENV-2013-6.2.1-Globaqua, the MASSTWIN project that has received funding from the European Union's Horizon 2020 research and innovation programme under grant agreement no. 692241 and by the Ministry of Higher Education, Science and Technology of the Republic of Slovenia (Programme group P1-0143). We thank Dr. Paul McGuinness for the language corrections and Dr. Petra Jenuš from Jožef Stefan Institute for providing TEM analysis of TiO₂NPs.

References

- [1] The Project of Emerging Nanotechnologies, Agrifood Nanotechnology Research and Development, <http://www.nanotechproject.org/inventories/> (Last accessed on 24th Feb. 2017).
- [2] A. Weir, P. Westerhoff, L. Fabricius, K. Hristovski, N. von Goetz, Titanium dioxide nanoparticles in food and personal care products, *Environ. Sci. Technol.* 46 (2012) 2242–2250.
- [3] G. Federici, B.J. Shaw, R.D. Handy, Toxicity of titanium dioxide nanoparticles to rainbow trout (*Oncorhynchus mykiss*): gill injury, oxidative stress, and other physiological effects, *Aquat. Toxicol.* 84 (2007) 415–430.
- [4] A. Menard, D. Drobne, A. Jemec, Ecotoxicity of nanosized TiO₂. Review of in vivo data, *Environ. Pollut.* 159 (2011) 677–684.

- [5] C. Som, P. Wick, H. Krug, B. Nowack, Environmental and health effects of nanomaterials in nanotextiles and façade coatings, *Environ. Int.* 37 (2011) 1131–1142.
- [6] W. Fan, M. Cui, H. Liu, C. Wang, Z. Shi, C. Tan, X. Yang, Nano-TiO₂ enhances the toxicity of copper in natural water to *Daphnia magna*, *Environ. Pollut.* 159 (2011) 729–734.
- [7] D.B. Warheit, T.R. Webb, K.L. Reed, S. Frerichs, C.M. Sayes, Pulmonary toxicity study in rats with three forms of ultrafine-TiO₂ particles: differential responses related to surface properties, *Toxicology* 230 (2007) 90–104.
- [8] C. Jin, Y. Tang, F.G. Yang, X.L. Li, S. Xu, X.Y. Fan, Y.Y. Huang, Y.J. Yang, Cellular toxicity of TiO₂ nanoparticles in anatase and rutile crystal phase, *Biol. Trace Elem. Res.* 141 (2011) 3–15.
- [9] K. Gerloff, I. Fenoglio, E. Carella, J. Kolling, C. Albrecht, A.W. Boots, I. Förster, R.P.F. Schins, Distinctive toxicity of TiO₂ rutile/anatase mixed phase nanoparticles on Caco-2 cells, *Chem. Res. Toxicol.* 25 (2012) 646–655.
- [10] F. Gottschalk, T. Sonderer, R.W. Scholz, B. Nowack, Modeled environmental concentrations of engineered nanomaterials (TiO₂, ZnO, Ag, CNT, fullerenes) for different regions, *Environ. Sci. Technol.* 43 (2009) 9216–9222.
- [11] G.E. Schaumann, A. Philippe, M. Bundschuh, G. Metreveli, S. Klitzke, D. Rakcheev, A. Grün, S.K. Kumahor, M. Kühn, T. Baumann, F. Lang, W. Manz, R. Schulz, H.-J. Vogel, Understanding the fate and biological effects of Ag- and TiO₂-nanoparticles in the environment: the quest for advanced analytics and interdisciplinary concepts, *Sci. Total Environ.* 535 (2014) 3–19.
- [12] R.F. Domingos, N. Tufenkji, K.J. Wilkinson, Aggregation of titanium dioxide nanoparticles: role of a fulvic acid, *Environ. Sci. Technol.* 43 (2009) 1282–1286.
- [13] F. Loosli, P. Le Coustumer, S. Stoll, Effect of electrolyte valency, alginate concentration and pH on engineered TiO₂ nanoparticle stability in aqueous solution, *Sci. Total Environ.* 535 (2015) 28–34.
- [14] I. López-Heras, Y. Madrid, C. Cámara, Prospects and difficulties in TiO₂ nanoparticles analysis in cosmetic and food products using asymmetrical flow field-flow fractionation hyphenated to inductively coupled plasma mass spectrometry, *Talanta* 124 (2014) 71–78.
- [15] V. Nischwitz, H. Goenaga-Infante, Improved sample preparation and quality control for the characterisation of titanium dioxide nanoparticles in sunscreens using flow field flow fractionation on-line with inductively coupled plasma mass spectrometry, *J. Anal. Atom. Spectrom.* 27 (2012) 1084–1092.
- [16] K. Tiede, A.B. Boxall, X. Wang, D. Gore, D. Tiede, M. Baxter, H. David, S.P. Tear, J. Lewis, Application of hydrodynamic chromatography-ICP-MS to investigate the fate of silver nanoparticles in activated sludge, *J. Anal. At. Spectrom.* 25 (2010) 1149–1154.
- [17] C. Tso, C. Zhung, Y. Shih, Y.-M. Tseng, S. Wu, R. Doong, Stability of metal oxide nanoparticles in aqueous solutions, *Water Sci. Technol.* 61 (2010) 127–133.
- [18] D.M. Mitrano, E.K. Leshner, A. Bednar, J. Monserud, C.P. Higgins, J.F. Ranville, Detecting nanoparticulate silver using single-particle inductively coupled plasma-mass spectrometry, *Environ. Toxicol. Chem.* 31 (2012) 115–121.
- [19] P.S. Fedotov, N.G. Vanifatova, V.M. Shkinev, B.Y. Spivakov, Fractionation and characterization of nano- and microparticles in liquid media, *Anal. Bioanal. Chem.* 400 (2011) 1787–1804.
- [20] C. Degueldre, P.-Y. Favarger, Thorium colloid analysis by single particle inductively coupled plasma-mass spectrometry, *Talanta* 62 (2004) 1051–1054.
- [21] C. Degueldre, P.-Y. Favarger, C. Bitea, Zirconia colloid analysis by single particle inductively coupled plasma-mass spectrometry, *Anal. Chim. Acta* 518 (2004) 137–142.
- [22] C. Degueldre, P.-Y. Favarger, S. Wold, Gold colloid analysis by inductively coupled plasma-mass spectrometry in a single particle mode, *Anal. Chim. Acta* 555 (2006) 263–268.
- [23] F. Laborda, J. Jiménez-Lamana, E. Bolea, J.R. Castillo, Critical considerations for the determination of nanoparticle number concentrations, size and number size distributions by single particle ICP-MS, *J. Anal. At. Spectrom.* 28 (2013) 1220–1232.
- [24] F. Laborda, J. Jiménez-Lamana, E. Bolea, J.R. Castillo, Selective identification, characterization and determination of dissolved silver(I) and silver nanoparticles based on single particle detection by inductively coupled plasma mass spectrometry, *J. Anal. At. Spectrom.* 26 (2011) 1362–1371.
- [25] X. Liu, G. Chen, C. Su, Effects of material properties on sedimentation and aggregation of titanium dioxide nanoparticles of anatase and rutile in the aqueous phase, *J. Colloid Interface Sci.* 363 (2011) 84–91.
- [26] R.B. Reed, C.P. Higgins, P. Westerhoff, S. Tadjiki, J.F. Ranville, Overcoming challenges in analysis of polydisperse metal-containing nanoparticles by single particle inductively coupled plasma mass spectrometry, *J. Anal. At. Spectrom.* 27 (2012) 1093–1100.
- [27] J. Tuoriniemi, G. Cornelis, M. Hassellöv, Size discrimination and detection capabilities of single-particle ICPMS for environmental analysis of silver nanoparticles, *Anal. Chem.* 84 (2012) 3965–3972.
- [28] A.P. Gondikas, P.F. von der Kammer, R.B. Reed, S. Wagner, J.F. Ranville, T. Hofmann, Release of TiO₂ nanoparticles from sunscreens into surface waters: a one-year survey at the Old Danube Recreational Lake, *Environ. Sci. Technol.* 48 (2014) 5415–5422.
- [29] A.R. Donovan, C.D. Adams, Y. Ma, C. Stephan, T. Eichholz, H. Shi, Single particle ICP-MS characterization of titanium dioxide, silver, and gold nanoparticles during drinking water treatment, *Chemosphere* 144 (2016) 148–153.
- [30] Y. Dan, H. Shi, C. Stephan, X. Liang, Rapid analysis of titanium dioxide nanoparticles in sunscreens using single particle inductively coupled plasma-mass spectrometry, *Microchem. J.* 122 (2015) 119–126.
- [31] J. Vidmar, R. Milačič, V. Golja, S. Novak, J. Ščančar, Optimization of the procedure for efficient dispersion of titanium dioxide nanoparticles in aqueous samples, *Anal. Methods* 8 (2016) 1194–1201.
- [32] M.D. Montañón, J.W. Olesik, A.G. Barber, K. Challis, J.F. Ranville, Single particle ICP-MS: advances toward routine analysis of nanomaterials, *Anal. Bioanal. Chem.* 408 (2016) 5053–5074.
- [33] A. Navarro-Ortega, V. Acuna, A. Bellin, P. Burek, G. Cassiani, R. Choukr-Allah, S. Dolédec, A. Elosegi, F. Ferrari, A. Ginebreda, P. Grathwohl, C. Jones, P.K. Rault, K. Kok, P. Koundouri, R.P. Ludwig, R. Merz, R. Milačič, I. Munoz, G. Nikulin, C. Paniconi, M. Paunović, M. Petrovic, L. Sabater, S. Sabater, N.T. Skoulikidis, A. Slob, G. Teutsch, N. Voulvoulis, D. Barceló, Managing the effects of multiple stressors on aquatic ecosystems under water scarcity, the GLOBAQUA project, *Sci. Total Environ.* 503–504 (2015) 3–9.
- [34] T.W. May, R.H. Wiedmeyer, A table of polyatomic interferences in ICP-MS, *At. Spectrosc.* 19 (1998) 150–155.
- [35] H.E. Pace, N.J. Rogers, C. Jarolimek, V.A. Coleman, C.P. Higgins, J.F. Ranville, Determining transport efficiency for the purpose of counting and sizing nanoparticles via single particle inductively coupled plasma mass spectrometry, *Anal. Chem.* 83 (2011) 9361–9369.
- [36] F. Laborda, E. Bolea, J. Jimenez-Lamana, Powerful tool for nanoanalysis, *Anal. Chem.* 86 (2014) 2270–2278.
- [37] S. Lee, X. Bi, R.B. Reed, J.F. Ranville, P. Herckes, P. Westerhoff, Nanoparticle size detection limits by single particle ICP-MS for 40 elements, *Environ. Sci. Technol.* 48 (2014) 10291–10300.
- [38] J.D. Hem, Study and interpretation of the chemical characteristics of natural water, *U. S. Geol. Surv. Water Supply Pap.* 2254 (1992) (263pp.).
- [39] G. Cornelis, M. Hassellöv, A signal deconvolution method to discriminate smaller nanoparticles in single particle ICP-MS, *J. Anal. At. Spectrom.* 29 (2014) 134.